Journal of the mechanical behavior of biomedical materials 69 (2017) 185–192

Contents lists available at ScienceDirect

Journal of the Mechanical Behavior of Biomedical Materials

journal homepage: www.elsevier.com/locate/jmbbm

Research Paper

Fatigue life of bovine meniscus under longitudinal and transverse tensile loading

Jaremy J. Creechley, Madison E. Krentz, Trevor J. Lujan*

Boise State University, 1910 University Drive, Boise, ID 83725-2085, United States

ARTICLE INFO

Keywords:
Meniscus
Fatigue
Failure
Collagen
Creep
Fracture

ABSTRACT

The knee meniscus is composed of a fibrous extracellular matrix that is subjected to large and repeated loads. Consequently, the meniscus is frequently torn, and a potential mechanism for failure is fatigue. The objective of this study was to measure the fatigue life of bovine meniscus when applying cyclic tensile loads either longitudinal or transverse to the principal fiber direction. Fatigue experiments consisted of cyclic loads to 60%, 70%, 80% or 90% of the predicted ultimate tensile strength until failure occurred or 20,000 cycles was reached. The fatigue data in each group was fit with a Weibull distribution to generate plots of stress level vs. cycles to failure (S-N curve). Results showed that loading transverse to the principal fiber direction gave a two-fold increase in failure strain, a three-fold increase in creep, and a nearly four-fold increase in cycles to failure (not significant), compared to loading longitudinal to the principal fiber direction. The S-N curves had strong negative correlations between the stress level and the mean cycles to failure for both loading directions, where the slope of the transverse S-N curve was 11% less than the longitudinal S-N curve (longitudinal: S=108–5.9ln(N); transverse: S=112–5.2ln(N)). Collectively, these results suggest that the non-fibrillar matrix is more resistant to fatigue failure than the collagen fibers. Results from this study are relevant to understanding the etiology of atraumatic radial and horizontal meniscal tears, and can be utilized by research groups that are working to develop meniscus implants with fatigue properties that mimic healthy tissue.

1. Introduction

The knee meniscus is a fibrocartilaginous soft tissue that distributes and dissipates cyclic loads across the tibiofemoral joint. By distributing loads, the meniscus helps protect the articular cartilage by reducing the peak stress transmitted across the cartilage surfaces by over two-fold (Wang et al., 2015). The meniscus performs this important function in an extreme mechanical environment that experiences sudden and recurring forces, and consequently the meniscus is one of the most frequently torn soft tissues in the body, with over 500,000 acute injuries in the U.S. each year (Kim et al., 2011). Tearing of the meniscus can cause pain, swelling, joint instability, and increased risk of developing osteoarthritis (McDermott and Amis, 2006; Makris et al., 2011; Roemer et al., 2009). Unfortunately, for most meniscus injuries, there is no effective treatment to fully restore meniscus function (Makris et al., 2011; Messner and Gao, 1998; Baker et al., 2002). Improvements in the treatment and prevention of meniscus injuries require an understanding of the failure mechanisms that cause tears to develop and propagate.

While meniscal tears are most commonly associated with a single high-magnitude loading event, there is evidence that meniscal tears may also develop from repeated exposure to low-magnitude loads, a phenomenon known as fatigue failure. These fatigue failures occur at stresses below the material strength, as repetitive loads cause micro-cracks to form and propagate to fracture. A recent study found that a third of patients with acute meniscus tears did not have a traumatic event or degenerative condition, and therefore the tears may be related to fatigue failure (Demange et al., 2016), while other studies have designated similar tear etiologies as atraumatic (Venkatachalam et al., 2001; Taylor et al., 2009). The existence of fatigue failure in soft fibrous tissue is further supported by numerous studies in tendon, which have demonstrated that low-magnitude repetitive loading will ultimately cause acute tendon failure (Schechtman and Bader, 1997; Schechtman and Bader, 2002; Fung et al., 2009; Thorpe et al., 2016). In order to identify loading patterns that lead to tendon overuse injuries, researchers have characterized tendon fatigue behavior using a stress-life method, whereby the number of cycles to failure is measured at variable stress levels (Schechtman and Bader, 1997).

To similarly characterize meniscus fatigue behavior, it's important to consider the anisotropic extracellular organization that enables the

* Corresponding author.
E-mail addresses: jaremycreechley@u.boisestate.edu (J.J. Creechley), maddiekrentz@u.boisestate.edu (M.E. Krentz), trevorlujan@boisestate.edu (T.J. Lujan).

http://dx.doi.org/10.1016/j.jmbbm.2016.12.020
Received 1 August 2016; Received in revised form 19 December 2016; Accepted 23 December 2016
Available online 27 December 2016

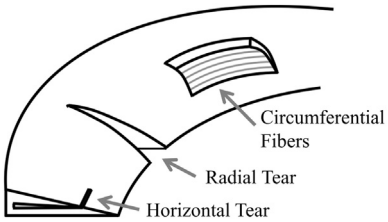

Fig. 1. Illustration of common meniscal tears and the principal fiber orientation.

meniscus to support large stresses. The meniscus extracellular matrix is structurally reinforced with a fibrous collagen network that makes up 75% of the dry weight (Makris et al., 2011). These collagen fibers are embedded in a ground substance that consists mostly of glycosaminoglycans, glycoproteins, elastin and water (McDevitt and Webber, 1990). In meniscus, the fibrous architecture displays a distribution of fiber orientations, where the majority of collagen fibers are aligned *longitudinal* to the meniscus circumference (Fig. 1), and a smaller subset of collagen fibers, called tie fibers (Andrews et al., 2014), are aligned *transverse* to the circumference. The circumferential collagen fibers provide the majority of the load distribution function, as these fibers resist deformation caused by the circumferential tensile stress or hoop stress generated in the semi-circular meniscus during joint compression (Messner and Gao, 1998). The generation of tensile strains during joint compression, both longitudinal and transverse to the circumferential fiber direction, have been experimentally verified using imaging technology (Kolaczek et al., 2016).

Failure patterns common to the meniscus relate to the anisotropic nature of the fibrous network. Radial tears account for approximately 5% to 15% of all meniscus tears and may occur when stresses longitudinal to the circumferential fiber direction cause tensile strains to exceed a failure limit (Fig. 1) (Metcalf and Barrett, 2004; Magee et al., 2002). Horizontal tears account for approximately 32% of all meniscal tears and may occur when stresses transverse to the circumferential fiber direction cause tensile strains to exceed a failure limit (Fig. 1) (Metcalf and Barrett, 2004). Although the stresses and strains that cause quasi-static failure of human and animal meniscus have been well characterized for quasi-static loading conditions, no study has yet characterized the tensile fatigue behavior of meniscus. Furthermore, to our knowledge, no study on soft connective tissue has directly measured the tensile fatigue behavior transverse to the principal collagen fiber orientation.

The objective of this study is to characterize the fatigue life of bovine meniscus under longitudinal and transverse tensile loading. This study aims to fill a current knowledge gap in the fatigue behavior of meniscus, and will determine if fiber orientation has any influence on fatigue properties.

2. Materials and methods

The stress-life fatigue behavior of bovine meniscus was characterized in two stages. In stage one, ultimate tensile stress (UTS) experiments were performed by straining specimens under quasi-static loading to failure. In stage two, fatigue experiments were performed on meniscus specimens by applying cyclic tensile stresses to either 60%, 70%, 80% or 90% of their predicted ultimate tensile strength (% UTS) until failure occurred or a maximum number of cycles was reached. Specimens were tested with fiber orientations aligned either longitudinal or transverse to the loading direction. This experimental design resulted in eight groups for fatigue testing, with four specimens in each group, for a total of 32 experiments. A Weibull distribution was used to fit the fatigue data in each group, and the mean value from these distributions was used to generate plots of stress level vs. cycles to failure (S-N curves).

2.1. Specimen preparation

The UTS and fatigue failure experiments were performed using meniscus specimens acquired from left and right hind bovine knees. Whole knees were obtained 1–2 days after sacrifice from a local abattoir (Greensfield, Meridian ID). They were stored at −20°C until they were dissected and the medial meniscus was harvested. Each whole meniscus was wrapped in gauze, which was moistened with saline solution, and was allowed to freeze thoroughly for a minimum of 1 day.

Frozen meniscus specimens were divided into three wedges using a hacksaw (Fig. 2A). Individual wedges from the posterior section were embedded in a composite of cellulose and saline solution and then packed in a small square plastic container (3.0 cm×3.0 cm). These embedded meniscus wedges were returned to the freezer within 1–3 h to minimize thawing. The reason for embedding the meniscus is that the cellulose media freezes into a solid cube and thereby provides planar surfaces that improve the slicing of the meniscus tissue into uniform layers.

The meniscus was layered using a commercial deli-slicer that was modified with a customized metal clamp system designed to rigidly hold each specimen cube during slicing (Globe, Bridgeport CT; Model C12). Vertical layers were sliced in zones 1 and 2 of the posterior meniscus region (Fig. 2 B), parallel to the circumferential fiber direction. The rationale for testing from this anatomical location, is that the highest incidence of horizontal and radial tears have been shown to occur in the medial meniscus in zones 1 and 2 (Metcalf and Barrett, 2004; Baker et al., 1985; Terzidis et al., 2006). Each meniscus wedge was sliced to a nominal thickness of 1.0 mm, and layers were allowed to thaw (Fig. 2B). This procedure allowed us to collect 10–15 layers per meniscus from zones 1–2.

The specimens were then cut into dumbbell shapes using custom razor punches (Fig. 2C). The long axis of the punches were oriented either longitudinal or transverse to the principal orientation of the visible fiber bundles. The central width of the punches was 1.0 mm, and the tab width for gripping to prevent slipping was set to 3.2 mm. The distance between the tabs was set to 14.0 and 7.0 mm for longitudinal

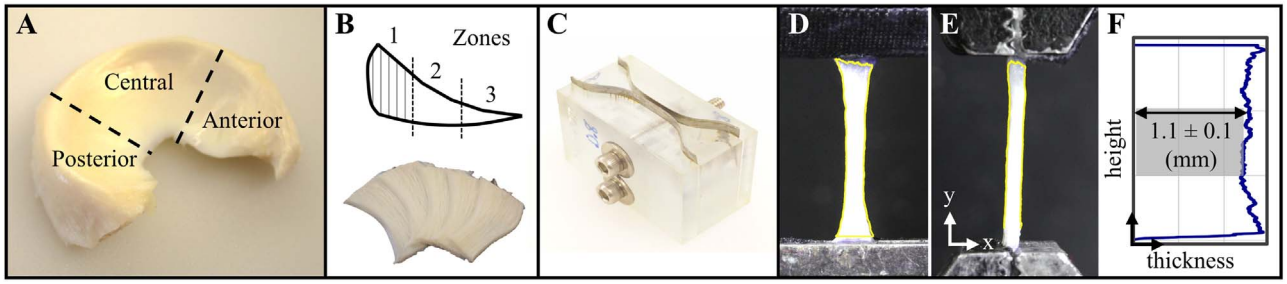

Fig. 2. Meniscus specimen preparation. A) Bovine meniscus was sectioned into regions, B) then vertically sliced into 1 mm thick layers and C) punched using a custom jig. D) Front and E) side dimensions were outlined using image-processing algorithms (yellow line). This protocol produced test specimens with G) consistent dimensions (grey box). (For interpretation of the references to color in this figure legend, the reader is referred to the web version of this article.)

Table 1
Physical dimensions of bovine test specimens.

Experiment	Fiber orientation	Length[a] (mm)	Width (mm)	Thickness (mm)	Intra-specimen variability in thickness (mm)
UTS	Longitudinal	14.5 ± 0.2	1.32 ± 0.13	1.22 ± 0.17	0.18 ± 0.04
	Transverse	8.1 ± 0.8	1.34 ± 0.07	1.03 ± 0.15	0.19 ± 0.04
Fatigue	Longitudinal	14.6 ± 0.2	1.20 ± 0.08	1.05 ± 0.11	0.14 ± 0.03
	Transverse	8.8 ± 1.1	1.08 ± 0.26	0.92 ± 0.19	0.17 ± 0.07

[a] Clamp-to-clamp; all values are mean ± standard deviation.

and transverse punches, respectively. The width to length aspect ratio of the razor punches was selected based on ASTM guidelines for tension-tension fatigue testing of matrix composite materials (ASTM 2002).

The actual dimensions of the meniscus specimens were calculated prior to UTS and fatigue experiments using a custom Python program to analyze digital images of each specimen. Images were taken at side and front profiles of every meniscus specimen using a mounted digital camera (UTS tests: Sony, New York NY, AS100V; Fatigue tests: Cannon, Melville NY, EOS T3i). The Python program used OTSU thresholding from scikit-image libraries to segment the front and side specimen profile (Fig. 2D and E) (Oliphant, 2007). The binary outlines from segmentation were analyzed to determine the average number of pixels that spanned the middle third of the gauge length to calculate specimen width and thickness from the front and side profiles, respectively (Fig. 2F). Pixels were converted to metric units using a two-dimensional calibration frame (1 pixel=~10 μm). This measurement technique enabled us to accurately calculate the inter- and intra-specimen variability of the specimen dimensions (Table 1).

2.2. Quasi-static failure

The UTS of bovine meniscus was characterized prior to running fatigue experiments. A total of 21 meniscus specimens from six unpaired hind bovine knees were quasi-statically loaded in uniaxial tension. Two UTS groups were tested based on fiber orientation: Longitudinal and transverse. All experiments were conducted using an electrodynamic test system (Instron, Norwood MA; ElectroPuls E10000). Specimens were cut into dumbbell shapes and imaged to measure specimen dimensions (Table 1) using previously described methods (see Section 2.1). Prior to imaging, specimens were preloaded to 0.50 N or 0.10 N for longitudinal and transverse tests, respectively. Specimens were then mechanically preconditioned with a 20 cycle triangular wave and a 20 cycle sinusoidal wave, both at 2 Hz and 8% clamp strain. After a 5 second rest, specimens were pulled to failure at 0.2 mm/s (Fig. 3A). The location of failure was documented and the stress-strain curve was analyzed to measure UTS and strain at failure. In addition, the linear modulus from preconditioning tests was calculated as the slope of the stress-strain curve from the 19th triangular wave cycle (Fig. 3B). The linear modulus was calculated using linear regression to fit a straight line between 6% and 8% clamp strain ($R^2 > 0.98$ for all tests).

2.3. Fatigue failure

To characterize fatigue life using a stress-life method, the UTS of a material must be known in order to measure the number of cycles to failure at a specific fatigue strength, which can be measured as a percentage of UTS (%UTS). A challenge in characterizing the stress-life for meniscus, or any soft heterogeneous tissue, is that large variations in UTS exist between specimens. These large inter-specimen variations preclude the reliable prediction of %UTS from a universal UTS value. To overcome this challenge, we created linear regression functions of the UTS and linear modulus values acquired during quasi-static testing. Importantly, these linear functions allowed us to non-destructively predict the UTS for each individual specimen by measuring the linear modulus prior to fatigue testing. This novel procedure enabled us to conduct fatigue tests based on %UTS, and to generate S-N curves for a highly heterogeneous material.

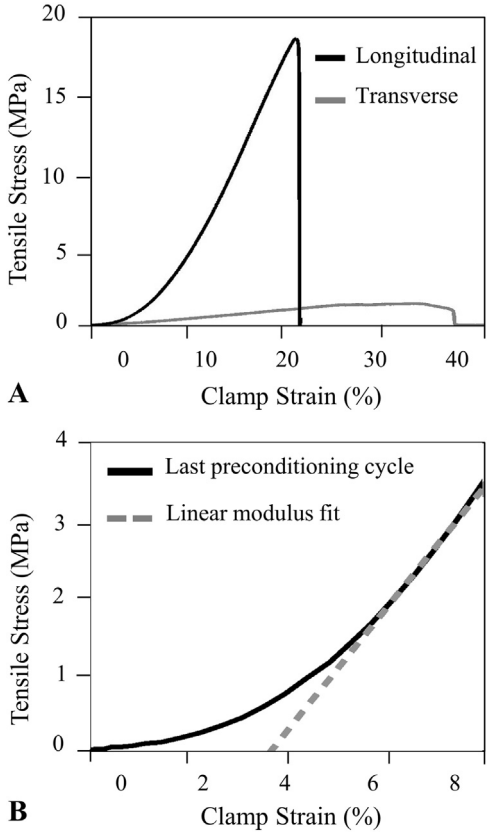

Fig. 3. Raw data from UTS experiments. A) Stress-strain curves during quasi-static loading to failure for a longitudinal and transverse specimen. B) Prior to failure, specimens were preconditioned and the linear modulus was calculated by fitting a line (dashed gray) to the linear region of the stress-strain curve.

The longitudinal and transverse fatigue life of bovine meniscus was characterized by testing a total of 32 specimens from 5 unpaired hind bovine knees in uniaxial tension. The posterior wedge from the medial meniscus provided on average 12 test specimens per knee (Fig. 2). Specimens were separated to ensure that all test groups had at least 3 specimens from different animals. Specimens were preloaded, imaged to determine dimensions, and preconditioned using the same methodology described for the UTS tests. Linear modulus was calculated from the 19th preconditioning cycle (Fig. 3B). As previously mentioned, the specimen-specific UTS was then predicted from the linear modulus, by using linear regression functions of UTS vs. linear modulus from quasi-static testing. Each specimen's predicted UTS was used to calculate the maximum stress magnitude at a specific %UTS (60%, 70%, 80% or 90%). This maximum stress magnitude was applied with a 2 Hz tension-tension sine wave that had a ratio of min force to max force set at 0.1 (Fig. 4A). To operate in load control, the Instron mechanical test system required an initial ramping of cyclic stress

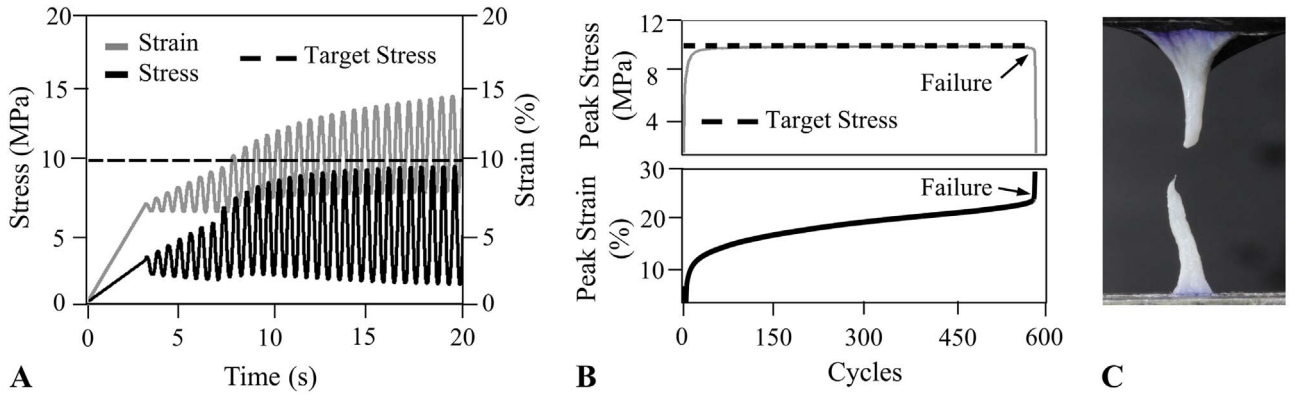

Fig. 4. Results from a fatigue experiment. A) Stress and strain response during initial fatigue loading to a target stress of 70% predicted UTS. B) Peak stress and peak strain values during cyclic fatigue loading of a transverse specimen. C) Image of a specimen after failure by fatigue loading.

(Fig. 4A), and the number of cycles to failure began to be counted once the peak cyclic stress reached 80% of the targeted stress. These cyclic stresses were maintained until specimen failure or a maximum number of 20,000 cycles was reached. The number of cycles to failure and specimen length at failure, l_f, was recorded using a failure criteria determined by a 25% loss of stress resistance (Fig. 4B). Failure strain was calculated using $(l_f\text{-}l_o)/l_o$, where l_o is initial specimen length and l_f is final specimen length. Creep was calculated by subtracting the length at failure l_f from the specimen length when the number of cycles to failure began to be counted. The location of failure was recorded using a digital camera, and was classified as midsubstance if it failed within the gauge length (Fig. 4C). During cyclic testing, tissue hydration was maintained using a drip of 9% saline solution at room temperature (average drip rate of 73 mL/min).

Results from all tests were reviewed to ensure that the actual maximum stress magnitude during cyclic testing, after reaching steady state, was within 5% of the targeted stress level (average difference between targeted stress and actual stress for all tests=−0.4 ± 2.8%). Due to large temperature fluctuations in the mechanical testing room, which influenced the accuracy of the load sensor during fatigue experiments, a total of sixteen specimens from four test groups were invalidated and new specimens were tested. During retesting, the problem was corrected by constructing an enclosed testing chamber that maintained air temperature to within 0.5 °C.

2.4. Statistical analysis

For quasi-static failure testing, the effect of fiber orientation on tangent modulus, UTS, and failure strain was assessed using a MANOVA. For fatigue failure testing, the effect of fiber orientation and maximum stress (%UTS) on tangent modulus, UTS (predicted), max stress (targeted), failure strain, and cycles-to-failure was assessed using a MANOVA, followed by Bonferroni post-hoc tests if significance was detected. The effect of fiber orientation on creep results was determined using an independent t-test.

Stress-life fatigue diagrams (S-N curves) were produced using a two-step process. In the first step, a two-parameter Weibull probability distribution was fit to the cycles-to-failure data for each test group using SAS analytical software (SAS Institute Inc., Cary NC). The mean, scaling parameter, shape parameter, and goodness of fit of the Weibull probability distribution function were calculated for each unique stress level and fiber orientation (eight groups total, sample size per group=4). Type-I right censoring was automatically applied in SAS software via the built-in maximum-likelihood estimation method for any run-out specimens, which were defined as specimens not failing before the fatigue test stopped at 20,000 cycles. In the second step, the mean values acquired from the Weibull probability distributions, representing the mean number of cylces before failure at each stress level, were plotted to generate S-N curves for longitudinal and transverse uniaxial tests. Regression analysis was performed on the S-N curves using linear, logarithmic and exponential functions to model the relationship between mean cycles to failure and stress level. The use of a Weibull probability distribution follows established methods for stress-life fatigue analysis of tendon (Schechtman and Bader, 1997), and the sample size of 16 specimens used to generate each S-N curve follows ASTM recommendations for tension-tension fatigue testing and statistical analysis (ASTM 2015).

3. Results

3.1. Quasi-static failure

There were significant differences in the experimental UTS results due to fiber orientation ($p < 0.001$). Specimens loaded transverse to the principal fiber orientation had a 93% decrease in UTS, a 96% decrease in linear modulus, and a 40% increase in failure strain (Table 2), compared to specimens loaded longitudinal to the principal fiber orientation. A strong positive correlation existed between the specimen UTS and linear modulus for specimens loaded longitudinal and transverse to the principal fiber orientation (Fig. 5). Of the twenty-one specimens tested for UTS, 7 failed at the midsubstance (central third), 11 failed between the midsubstance and clamps, and 3 specimens failed at the clamps.

3.2. Fatigue failure

The fatigue failure behavior of the medial meniscus was influenced by fiber orientation, but not the stress level (Table 3; $p < 0.001$ and $p=0.6$, respectively). Compared to specimens loaded longitudinal to the principal fiber direction, transverse specimens had a two-fold increase in failure strain ($p < 0.001$), and a nearly four-fold increase in cycles to failure (not significant, $p=0.12$). The transverse specimens also had three-fold greater creep than the longitudinal specimens (transverse creep=32 ± 17%, longitudinal creep=11 ± 8%; $p=0.001$). For transverse specimens, lower stress levels were associated with greater failure strains, but this trend was not significant ($p=0.4$). There was also not a significant effect of fiber orientation or stress level on cycles to failure

Table 2
Material properties from quasi-static failure experiments.

Fiber orientation	Linear modulus (MPa)	UTS (MPa)	Failure strain[a] (%)
Longitudinal	137.5 ± 49.8	19.4 ± 6.8	22.1 ± 3.0
Transverse	5.0 ± 3.3*	1.3 ± 0.9*	30.8 ± 5.6*

* Significantly different than the longitudinal fiber orientation ($p < 0.001$).
[a] Clamp-to-clamp strain.

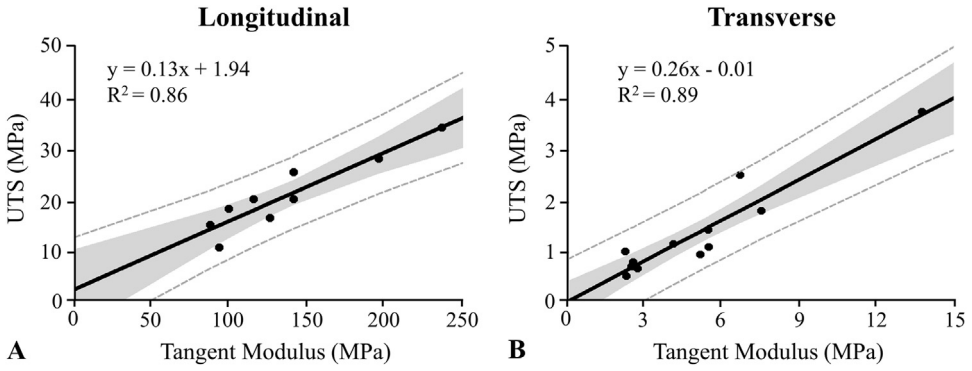

Fig. 5. Correlation of UTS and linear modulus from medial meniscus specimens that were quasi-statically loaded A) longitudinal and B) transverse to the principal fiber orientation. Gray region=95% confidence in linear fit, dashed line=95% confidence in UTS prediction.

(p=0.17 and p=0.12, respectively). Similar to our quasi-static testing results (Table 2), the linear modulus and UTS (predicted) of the transverse fatigue specimens were 94% and 88% less than the longitudinal fatigue specimens, respectively (Table 3). Of the thirty-two specimens tested for fatigue failure, 12 failed at the midsubstance (central third), 18 failed between the midsubstance and clamps, and 2 specimens failed at the clamps.

The Weibull probability distribution function produced good correlations to the fatigue failure results. At each stress level, positive linear correlations existed between the number of cycles to failure and failure risk (unreliability), with R^2 values of 0.80 ± 0.18 (Table 4). When plotting the S-N curves for longitudinal or transverse groups, strong negative linear-log correlations existed between the stress level and the mean cycles to failure (Fig. 6). The slope for the transverse S-N curve was 11% less than the slope of the longitudinal S-N curve. The y-intercepts of the S-N curves are an estimate of static strength, and therefore the S-N curves gave static strength values within 8% and 12% of the predicted static strength for the longitudinal and transverse specimens, respectively. The correlation of cycles to failure and unreliability was improved using linear and exponential functions, as they both gave fits with R^2 values of 0.83 and 0.93 for the longitudinal and transverse results, respectively.

Table 4
Parameters from Weibull probability distribution function.

Fiber orientation	Stress level (%UTS)	Scale η	Shape β	Mean	R^2
Longitudinal	90	21.8	0.48	47.3	0.72
	80	45.9	0.81	51.7	0.99
	70	977.8	0.60	1482.1	0.82
	60	853.1	0.52	1606.8	0.86
Transverse	90	19.6	0.45	48.6	0.50
	80	413.8	0.38	1536.1	0.92
	70	396	0.28	5097.8	0.61
	60	2332.2	0.45	5845.2	1.0

4. Discussion

The characterization of fatigue behavior has been critical to the description and prevention of failures in engineered structures that are subjected to cyclic loading (Bhaumik et al., 2008; Ritchie, 1999). Despite the fact that the meniscus experiences cyclic loads and a high rate of failure, the fatigue behavior of the meniscus has been poorly characterized. In this study, we have developed a novel methodology to measure the anisotropic fatigue behavior of soft fibrous tissues, and we have reported for the first time the in-vitro fatigue life of meniscus under tensile loading.

A principal finding of this study is that the stress-life fatigue behavior of the meniscus is dependent on fiber orientation. Specimens loaded transverse to the principal fiber orientation had on average two-fold greater failure strains, three-fold greater creep, and a four-fold greater number of cycles-to-failure, although the cycles-to-failure results were not significant (p=0.12). These results indicate that the non-fibrillar ground substance is more fatigue resistant than the collagen network, since the non-fibrillar ground substance supports a larger percentage of stress in specimens loaded transverse to the principal fiber orientation. The creep to failure behavior may offer additional insight, as the greater creep in the transverse specimens suggests that the ground substance and tie fibers are able to accrue considerable damage before catastrophic failure. Another possibility is that the transverse meniscus specimens are able to dissipate more energy during cyclic loading, however, viscoelastic tensile testing of ligament found no difference in energy dissipation properties between transverse and longitudinal specimens (Bonifasi-Lista et al., 2005).

This study may provide insight into meniscal tears that are

Table 3
Material properties from fatigue failure experiments.

Fiber orientation	Stress level (%UTS)	Linear modulus (MPa)	UTS, predicted (MPa)	Max stress, targeted (MPa)	Failure strain (%)[a]	Cycles to failure
Longitudinal	90	82.9 ± 27.9	12.3 ± 3.5	11.1 ± 3.2	20.7 ± 9.4	114 ± 221
	80	101.8 ± 70.9	14.7 ± 9.0	11.8 ± 7.2	18.6 ± 4.1	46 ± 48
	70	112.8 ± 33.6	16.1 ± 4.3	11.3 ± 3.0	21.2 ± 4.6	2155 ± 3851
	60	74.1 ± 23.0	11.2 ± 2.9	6.7 ± 1.7	24.1 ± 11.2	2424 ± 4551
	All	**92.9 ± 41.7**	**13.6 ± 5.3**	**10.2 ± 4.4**	**21.1 ± 7.4**	**1185 ± 2904**
Transverse	90	5.5 ± 0.7	1.4 ± 0.2	1.3 ± 0.2	34.4 ± 14.6	381 ± 759
	80	4.4 ± 1.2	1.2 ± 0.3	0.9 ± 0.3	41.3 ± 7.6	1801 ± 3469
	70	4.0 ± 1.4	1.1 ± 0.4	0.7 ± 0.3	46.6 ± 25.0	5976 ± 10,089
	60	4.0 ± 1.1	1.1 ± 0.3	0.6 ± 0.2	56.2 ± 17.1	10,598 ± 11,974
	All	**4.5 ± 1.2**[*]	**1.2 ± 0.3**[*]	**0.9 ± 0.3**[*]	**44.6 ± 17.5**[*]	**4689 ± 8275**

[*] Significantly different than longitudinal fiber orientation ($p < 0.001$).
[a] Clamp-to-clamp strain.

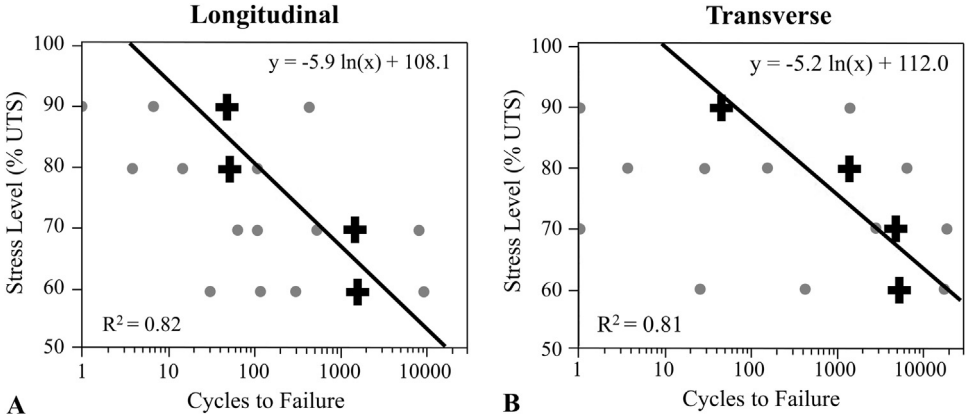

Fig. 6. Correlation of UTS and linear modulus from specimens tested A) longitudinal and B) transverse to the preferred fiber direction. Gray dots=cycles to failure for each specimen; Black cross=mean cycles to failure at each stress level (mean values from Weibull fit).

observed clinically. Common meniscal tear patterns include radial, horizontal, longitudinal (vertical), complex, flap, and bucket handle tears (Metcalf and Barrett, 2004). The longitudinal specimens tested in this study can relate to radial tear patterns, and therefore our fatigue results are relevant to a clinical study that found 32% of 435 patients with isolated meniscus tears, mostly radial, had symptoms consistent with fatigue failure (i.e. atraumatic with acute pain onset) (Demange et al., 2016). Results from the present study confirm that meniscal tissue is susceptible to radial fatigue failure, and that the circumferential fibers that resist radial tears appear more prone to fatigue than the non-fibrillar matrix. The transverse specimens tested in this study can relate to horizontal and longitudinal tear patterns, which both occur transverse to the principal fiber orientation and are two of the most common meniscal tears. Although horizontal tears are often asymptomatic, they can propagate to debilitating flap tears (Christoforakis et al., 2005; Yim et al., 2013). Longitudinal tears are associated with traumatic events and can propagate to bucket handle tears that restrict full extension of the knee joint. To our knowledge, no clinical study has yet directly linked horizontal or longitudinal tears to fatigue failure, but considering the high incidence of these tears in older adults and the low level of cyclic stresses that caused fatigue fracture in our transverse specimens (< 1 MPa), fatigue may be a potential failure mechanism.

Results from the fatigue tests can be compared to previous work. First, the fatigue life from our longitudinal and transverse meniscus specimens had a slope that was less than half that of human extensor digitorum longus tendon (meniscus=−5.9, tendon=−14.8). This would indicate that the bovine meniscus is more resistant to fatigue failure than human tendon. Second, the *in vitro* tensile strains measured in the present study are much greater than the *in vivo* tensile strains that occur during normal physiological loading. A study by Jones et al. used strain gauges in cadavers to find average circumferential tensile strains to be 2.7% under 3x body weight (Jones et al., 1996), while Kolaczek et al. imaged kinematic markers in cadavers using computed tomography to find that circumferential and superior-inferior strains could reach on average 4% tensile strain in certain locations under 1x body weight. The circumferential and superior-inferior tensile strains measured in these cadaveric studies correspond to the longitudinal and transverse tensile strains measured in the present study, respectively. By using the linear modulus we measured during quasi-static testing, a 4% strain is estimated to produce stresses of 3 Mpa and 0.1 Mpa for longitudinal and transverse uniaxial specimens, respectively. Therefore, to simulate physiological loads at 1x body weight, fatigue tests would need to be performed at 15% and 8% of the UTS for longitudinal and transverse specimens, respectively. Our fatigue experiments were limited to 20,000 cycles and 60% of the UTS, and therefore our results can only directly address the risk of fatigue failure during elevated loading events. This comparison with previous cadaveric meniscus studies is useful for comprehending our results, but any stress calculations made from cadaveric strains should be interpreted with caution, as cadaveric studies likely underestimate meniscus strain relative to our study. The reason being that different reference configurations are used to calculate strain, as strains measured in the cadaveric studies are referenced from a neutral position that includes the *in situ* stresses that naturally exist *in vivo*, while strains measured in the present study are referenced from a state of nearly zero stress.

The loading conditions we applied to characterize fatigue failure are notably different than physiological loading conditions. The present study used uniaxial tensile tests of thinly sectioned coupons, which is a simplification of the stress state that exists *in vivo*, where compressive loads to the knee joint create circumferential hoop stresses in the meniscus. This *in vivo* loading condition would subject stress elements in the meniscus to *plane stress*, with tensile and compressive stresses on perpendicular surfaces. As a result, cadaveric specimens would experience greater von Mises stress than if simply loaded in uniaxial tension. Since von Mises stress is a measure of distortion-energy and is used to predict yielding in ductile materials, it's conceivable that *in vivo* fatigue would occur at lower tensile strain values than we measured using uniaxial tensile tests.

Results from the quasi-static tests can also be compared to previous work. Our linear modulus values compared well to previous research, as our results were within 5% of the 140 MPa and 5 MPa reported by Proctor et al. for the longitudinal and radial modulus of bovine medial meniscus, respectively (Proctor et al., 1989). Our UTS results were within 5% of the 18.9 MPa longitudinal UTS reported by Danso et al. for bovine medial meniscus (Danso et al., 2014), and were within 40% of the 2.0 MPa transverse UTS reported by Tissakht and Ahmet for human meniscus (Tissakht and Ahmed, 1995). Our results were considerably lower than a study by Peloquin et al., which tested bovine medial meniscus and measured the longitudinal and transverse linear modulus to be 215 MPa and 17 MPa, respectively, and the longitudinal and transverse UTS to be 17 MPa and 4 MPa, respectively (Peloquin et al., 2016). The reason for our lower values may be due to differences in specimen geometry and differences in the methodology used to curve fit the linear modulus.

This study may be helpful to scientists and engineers that are designing meniscal replacement devices. An obstacle in the development of functional meniscus implants has been fatigue failure during long duration animal studies (Kelly et al., 2007; Hannink et al., 2011). To improve fatigue properties, researchers have begun to evaluate fatigue life of synthetic soft-tissue analogs, typically under compressive loading (Miller et al., 2016; Shemesh et al., 2014). The present study will allow research groups to directly compare the tensile fatigue properties of their replacement devices to the tensile fatigue properties

of native meniscus. Our evaluation of longitudinal and transverse fatigue life may be particularly useful for research groups that are engineering polymer composites to mimic the anisotropic fibrous matrix of native meniscus (Shemesh et al., 2014).

Another important contribution of this study is that a strong positive correlation was found to exist between the ultimate tensile strength (UTS) and the linear modulus of the meniscus. This correlation influenced the design of our fatigue experiments by allowing us to non-destructively predict the UTS for each specimen, and then to prescribe the peak loading magnitude during fatigue testing based on % UTS. This specimen-specific approach diverged from previous fatigue studies of tendon, which prescribed the peak loading magnitude based on a universal or average UTS value (Schechtman and Bader, 1997; Andarawis-Puri and Flatow, 2011). Although using an average UTS value would have simplified our fatigue testing protocol, and is recommended by ASTM standards for polymer matrix composites (ASTM 2002), the high inter-specimen variability of meniscus hindered this global approach. For example, the coefficient of variation of the UTS for tendon specimens used in previous fatigue experiments was 12% (Schechtman and Bader, 1997), while the coefficient of variation of the UTS for our transverse meniscus specimens was 70%. Consequently, if we used an average UTS value, we would have miscalculated the actual UTS during quasi-static testing by on average 60% per specimen. This large absolute error may explain why our preliminary tests that used an average UTS value for transverse fatigue tests were resulting in either immediate failure or no failure (data not shown). Alternatively, by using the linear correlation between linear modulus and UTS, our error in predicting the actual UTS for transverse quasi-static tests dropped to 19% per specimen, and using this alternative approach, our fatigue tests resulted in an S-N curve with variable failure durations (Fig. 6). Future fatigue studies could further improve confidence in predicting UTS by only testing specimens with a linear modulus in a range that corresponds to the tightest 95% confidence interval (Fig. 5, dashed lines). To our knowledge, the correlation between linear modulus and UTS has not been previously reported for meniscus tissue, but has been reported for human tendon (Matson et al., 2012) and bone (Hernandez et al., 2014; Zioupos and Currey, 1998).

Limitations existed with this study. We only tested the peripheral region of the medial meniscus, and fatigue properties may vary in different regions (e.g. lateral meniscus). Another limitation is the use of bovine meniscus as a surrogate for human tissue. Although bovine and human meniscus have similar structure and mechanical properties (Sweigart et al., 2004; Abraham et al., 2011), differences may exist in fatigue properties and our results should be interpreted accordingly. For this experiment, we examined fatigue life from tensile loads, as tensile strains occur during joint compression (Athanasiou and Sanchez-Adams, 2009), but fatigue failures may also occur from compressive strains. A sample size of four was used for each test group, which will limit the certainty of mean fatigue life at each stress level (Fig. 6). Despite the small sample size, the Weibull distribution had strong positive correlations in predicting risk of failure in six of the eight test groups (Table 4), and the sample size of 16 for each S-N curve exceeded ASTM standards for tension-tension fatigue testing and analysis (ASTM 2002; ASTM 2015). Finally, there are inherent limitations in using *in vitro* testing to characterize the fatigue behavior of meniscus, as we do not account for the mechanobiological responses that occur *in vivo*. Nevertheless, the in-vitro fatigue life reported in this study can serve as a baseline for the fatigue behaviors that may exist *in-vivo*, and this study can benefit researchers that wish to estimate the rate of healing needed to repair microtrauma induced by cyclic loading (Schechtman and Bader, 1997; Taylor and Lee, 2003).

5. Conclusions

The anisotropic fatigue life of bovine meniscus was characterized at stress levels between 60% and 90% of the ultimate tensile strength. The meniscus was more resistant to fatigue failure when loaded transverse to the principal fiber direction, as the ground substance and tie fibers withstood very large creeps, of on average 32%, before catastrophic failure. To measure the fatigue life of soft tissue with large variations in UTS, this study developed an experimental methodology to predict a specimen's UTS based on linear modulus. This novel method may be useful for characterizing fatigue life in other soft heterogeneous tissues. Results from this study suggest that repeated loading at stress magnitudes below the material strength is a potential failure mechanism for common meniscal tears (radial and horizontal), and future research is warranted to determine the prevalence of fatigue induced injuries in fibrocartilage, and strategies to prevent structural damage caused by repeated loading.

Acknowledgements

This material is based upon work supported by the National Science Foundation under grant no. 1554353, and the National Institute of General Medical Sciences of the National Institutes of Health under grant no. P20GM109095. Kind thanks to Phil Boysen and Greenfield Packing.

References

(ASTM), 2002. Standard Test Method for Tension-Tension Fatigue of Polymer Matrix Composite Materials. D 3479/D 3479M - 96 (2002). ASTM International, West Conshohocken, PA.
(ASTM), 2015. Standard Practice for Statistical Analysis of Linear or Linearized Stress-Life and Strain-Life Fatigue Data. ASTM E739-10.
Abraham, A.C., Edwards, C.R., Odegard, G.M., et al., 2011. Regional and fiber orientation dependent shear properties and anisotropy of bovine meniscus. J. Mech. Behav. Biomed. Mater. 4, 2024–2030.
Andarawis-Puri, N., Flatow, E.L., 2011. Tendon fatigue in response to mechanical loading. J. Musculoskelet. Neuronal Interact. 11, 106–114.
Andrews, S.H., Rattner, J.B., Abusara, Z., et al., 2014. Tie-fibre structure and organization in the knee menisci. J. Anat. 224, 531–537.
Athanasiou KA, Sanchez-Adams J., 2009. Engineering the Knee Meniscus: Morgan & Claypool.
Baker, B.E., Peckham, A.C., Pupparo, F., et al., 1985. Review of meniscal injury and associated sports. Am. J. Sports Med. 13, 1–4.
Baker, P., Coggon, D., Reading, I., et al., 2002. Sports injury, occupational physical activity, joint laxity, and meniscal damage. J. Rheumatol. 29, 557–563.
Bhaumik, S.K., Sujata, M., Venkataswamy, M.A., 2008. Fatigue failure of aircraft components. Eng. Fail. Anal. 15, 675–694.
Bonifasi-Lista, C., Lake, S.P., Small, M.S., et al., 2005. Viscoelastic properties of the human medial collateral ligament under longitudinal, transverse and shear loading. J. Orthop. Res.: Off. Publ. Orthop. Res. Soc. 23, 67–76.
Christoforakis, J., Pradhan, R., Sanchez-Ballester, J., et al., 2005. Is there an association between articular cartilage changes and degenerative meniscus tears? Arthrosc.: J. Arthrosc. Relat. Surg.: Off. Publ. Arthrosc. Assoc. N. Am. Int. Arthrosc. Assoc. 21, 1366–1369.
Danso, E.K., Honkanen, J.T., Saarakkala, S., et al., 2014. Comparison of nonlinear mechanical properties of bovine articular cartilage and meniscus. J. Biomech. 47, 200–206.
Demange, M.K., Gobbi, R.G., Camanho, G.L., 2016. "Fatigue meniscal tears": a description of the lesion and the results of arthroscopic partial meniscectomy. Int. Orthop. 40, 399–405.
Fung, D.T., Wang, V.M., Laudier, D.M., et al., 2009. Subrupture tendon fatigue damage. J. Orthop. Res.: Off. Publ. Orthop. Res. Soc. 27, 264–273.
Hannink, G., van Tienen, T.G., Schouten, A.J., et al., 2011. Changes in articular cartilage after meniscectomy and meniscus replacement using a biodegradable porous polymer implant. Knee Surg. Sports Traumatol. Arthrosc.: Off. J. ESSKA 19, 441–451.
Hernandez, C.J., Lambers, F.M., Widjaja, J., et al., 2014. Quantitative relationships between microdamage and cancellous bone strength and stiffness. Bone 66, 205–213.
Jones, R.S., Keene, G.C., Learmonth, D.J., et al., 1996. Direct measurement of hoop strains in the intact and torn human medial meniscus. Clin. Biomech. 11, 295–300.
Kelly, B.T., Robertson, W., Potter, H.G., et al., 2007. Hydrogel meniscal replacement in the sheep knee: preliminary evaluation of chondroprotective effects. Am. J. Sports Med. 35, 43–52.
Kim, S., Bosque, J., Meehan, J.P., et al., 2011. Increase in outpatient knee arthroscopy in the United States: a comparison of National Surveys of Ambulatory Surgery, 1996 and 2006. J. Bone Jt. Surg. Am. 93, 994–1000.
Kolaczek, S., Hewison, C., Caterine, S., et al., 2016. Analysis of 3D Strain in the Human Medial Meniscus. J. Mech. Behav. Biomed. Mater., 6.
Magee, T., Shapiro, M., Williams, D., 2002. MR accuracy and arthroscopic incidence of

meniscal radial tears. Skeletal Radiol. 12, 686–689.
Makris, E.A., Hadidi, P., Athanasiou, K.A., 2011. The knee meniscus: structure-function, pathophysiology, current repair techniques, and prospects for regeneration. Biomaterials 32, 7411–7431.
Matson, A., Konow, N., Miller, S., et al., 2012. Tendon material properties vary and are interdependent among turkey hindlimb muscles. J. Exp. Biol. 215, 3552–3558.
McDermott, I.D., Amis, A.A., 2006. The consequences of meniscectomy. J. Bone Jt. Surg. Br. 88, 1549–1556.
McDevitt, C.A., Webber, R.J., 1990. The ultrastructure and biochemistry of meniscal cartilage. Clin. Orthop. Relat. Res., 8–18.
Messner, K., Gao, J., 1998. The menisci of the knee joint. Anatomical and functional characteristics, and a rationale for clinical treatment. J. Anat. 193 (Pt 2), 161–178.
Metcalf, M.H., Barrett, G.R., 2004. Prospective evaluation of 1485 meniscal tear patterns in patients with stable knees. Am. J. Sports Med. 32, 675–680.
Miller, A.T., Safranski, D.L., Smith, K.E., et al., 2016. Compressive cyclic ratcheting and fatigue of synthetic, soft biomedical polymers in solution. J. Mech. Behav. Biomed. Mater. 54, 268–282.
Oliphant, T.E., 2007. Python for scientific computing. Comput. Sci. Eng. 9, 10–20.
Peloquin, J.M., Santare, M.H., Elliott, D.M., 2016. Advances in Quantification of Meniscus Tensile Mechanics Including Nonlinearity, Yield, and Failure. J. Biomech. Eng. 138, 021002.
Proctor, C.S., Schmidt, M.B., Whipple, R.R., Kelly, M.A., Mow, V.C., 1989. Material properties of the normal medial bovine meniscus. J. Orthop. Res. 7, 771–782.
Ritchie, R.O., 1999. Mechanisms of fatigue-crack propagation in ductile and brittle solids. Int. J. Fract. 100, 55–83.
Roemer, F.W., Guermazi, A., Hunter, D.J., et al., 2009. The association of meniscal damage with joint effusion in persons without radiographic osteoarthritis: the Framingham and MOST osteoarthritis studies. Osteoarthr. Cartil. OARS Osteoarthr. Res. Soc. 17, 748–753.
Schechtman, H., Bader, D.L., 1997. In vitro fatigue of human tendons. J. Biomech. 30, 829–835.
Schechtman, H., Bader, D.L., 2002. Fatigue damage of human tendons. J. Biomech. 35, 347–353.
Shemesh, M., Asher, R., Zylberberg, E., et al., 2014. Viscoelastic properties of a synthetic meniscus implant. J. Mech. Behav. Biomed. Mater. 29, 42–55.
Sweigart, M.A., Zhu, C.F., Burt, D.M., et al., 2004. Intraspecies and interspecies comparison of the compressive properties of the medial meniscus. Ann. Biomed. Eng. 32, 1569–1579.
Taylor, D., Lee, T.C., 2003. Microdamage and mechanical behaviour: predicting failure and remodelling in compact bone. J. Anat. 203, 203–211.
Taylor TL, Frankovich R, Rumball J., 2009. Bilateral atraumatic medial meniscal tears in a 17-year-old rower. BMJ Case Reports 2009.
Terzidis, I.P., Christodoulou, A., Ploumis, A., et al., 2006. Meniscal tear characteristics in young athletes with a stable knee: arthroscopic evaluation. Am. J. Sports Med. 34, 1170–1175.
Thorpe, C.T., Riley, G.P., Birch, H.L., et al., 2016. Fascicles and the interfascicular matrix show adaptation for fatigue resistance in energy storing tendons. Acta Biomater..
Tissakht, M., Ahmed, A.M., 1995. Tensile stress-strain characteristics of the human meniscal material. J. Biomech. 28, 411–422.
Venkatachalam, S., Godsiff, S.P., Harding, M.L., 2001. Review of the clinical results of arthroscopic meniscal repair. Knee 8, 129–133.
Wang, H., Chen, T., Gee, A.O., et al., 2015. Altered regional loading patterns on articular cartilage following meniscectomy are not fully restored by autograft meniscal transplantation. Osteoarthr. Cartil. OARS Osteoarthr. Res. Soc. 23, 462–468.
Yim, J.H., Seon, J.K., Song, E.K., et al., 2013. A comparative study of meniscectomy and nonoperative treatment for degenerative horizontal tears of the medial meniscus. Am. J. Sports Med. 41, 1565–1570.
Zioupos, P., Currey, J.D., 1998. Changes in the stiffness, strength, and toughness of human cortical bone with age. Bone 22, 57–66.